

Universal criterion and phase diagram for switching a magnetic vortex core in soft magnetic nanodots

Ki-Suk Lee,¹ Sang-Koog Kim,^{1*} Young-Sang Yu,¹ Youn-Seok Choi,¹ Konstantin Yu. Guslienko,¹

Hyunsung Jung,¹ and Peter Fischer²

¹*Research Center for Spin Dynamics and Spin-Wave Devices, and Nanospinics Laboratory, Department of Materials Science and Engineering, College of Engineering, Seoul National University, Seoul 151-744, Republic of Korea*

²*Center for X-Ray Optics, Lawrence Berkeley National Laboratory, 1 Cyclotron Road, Mail Stop 2R0400, Berkeley, California 94720, USA*

The universal criterion for ultrafast vortex-core switching between the up- and down-core bistates in soft magnetic nanodots was investigated by micromagnetic simulations along with analytical calculations. Vortex-core switching occurs whenever the velocity of vortex-core motion reaches the critical velocity that is expressed as $v_{\text{cri}} = \frac{5}{3} \gamma \sqrt{A_{\text{ex}}}$ (e.g. $v_{\text{cri}} = 330 \pm 37$ m/s for Permalloy), where A_{ex} is the exchange stiffness, and γ is the gyromagnetic ratio. On the basis of the above results, phase diagrams for the vortex-core switching event and switching times with respect to both the amplitude and frequency of applied *circularly rotating* magnetic field were calculated, which offer practical guidance for implementing nanodots in vortex states into future solid-state information-storage devices.

In magnetic thin films [1,2] and patterned magnetic elements of micrometer (or smaller) lateral size [3], a nontrivial, non-uniform magnetization (\mathbf{M}) configuration has been experimentally observed in both static and dynamic states. This magnetic nanostructure, the so-called “magnetic vortex”, has an in-plane curling \mathbf{M} along with an out-of-plane \mathbf{M} at the core area stretching over a few tens of nm in size [3]. Owing to a high thermal stability of this static structure as well as the bistate \mathbf{M} orientations of the tiny vortex core (VC), the magnetic vortex has been received considerable attention as an information carrier of binary digits “0” and “1” in future nonvolatile information-storage devices [4]. Furthermore, very recently, experimental, theoretical, and simulation studies have explored a rich variety of the dynamic properties of the magnetic vortex, including ultrafast VC switching by linearly oscillating [5-7] and circularly rotating [8-10] in-plane magnetic fields or spin-polarized ac currents [11,12], with extremely low power consumption. The underlying mechanism and physical origin of ultrafast VC switching have also been found [5-7,13]. These rich dynamic properties stimulate continuing intensive studies of patterned magnetic elements in vortex states targeting towards a fundamental understanding of their dynamics [6,7,11,13,14] and real applications to a new class of nonvolatile random access memory [15] and patterned information storage media [4,9]. Such new conceptual devices using ultrafast, low-power VC switching becomes an emerging key issue in the research areas of nanomagnetism and \mathbf{M} dynamics. Although, the fundamental understanding of the VC reversal and vortex gyrotropic dynamics were much advanced recently,

the universal criterion for VC switching, its phase diagram, and switching time have not been investigated yet. Moreover, these are technologically essential parameters for a reliable manipulation of the VC switching acting as a basic function in information-storage devices, which should be identified for its practical applications.

In this Letter, we report on the universal criterion, namely the critical velocity v_{cri} of VC motions required for VC switching, as found by micromagnetic simulations and analytical calculations. On the basis of the universality of v_{cri} we derive phase diagrams of the VC reversal event and switching times with respect to the amplitude and frequency of *circularly rotating* magnetic field.

In the present study, the OOMMF code [16] was used that utilizes the Landau-Lifshitz-Gilbert (LLG) equation of motion [17] because this approach is a well established, optimized tool, and reliable enough to investigate \mathbf{M} dynamics on a few nm spatial and > 10 ps temporal scales. In addition, we used an analytical approach to determine the threshold of driving forces required for VC switching and necessary switching time, based on the linearized Thiele's equation [18] of motion. We used Permalloy (Py: $\text{Ni}_{80}\text{Fe}_{20}$) nanodots as a model system, each dot with a different radius R ranging from 150 to 600 nm and a different thickness L ranging from 10 to 50 nm [see Fig. 1(a)].

To excite vortex gyrotropic motions up to the VC switching, we used a specially designed driving force of counter-clockwise (CCW) circularly rotating magnetic fields in the dot

plane with the angular frequency $\omega_{\mathbf{H}}$ and the amplitude H_0 , denoted as $\mathbf{H}_{\text{CCW}} = H_0 [\cos(\omega_{\mathbf{H}}t)\hat{\mathbf{x}} + \sin(\omega_{\mathbf{H}}t)\hat{\mathbf{y}}]$ [19,20]. The reason for selecting this \mathbf{H}_{CCW} is that it is most effective for selective resonant excitations of only the core-up vortex state, as demonstrated in earlier theoretical and simulation works [9,20], and in recent experimental work [10]. An example of the resonant vortex gyrotropic motion and VC switching driven by \mathbf{H}_{CCW} with $H_0 = 20$ Oe and $\nu_{\mathbf{H}} = \omega_{\mathbf{H}}/2\pi = 580$ MHz (where $\nu_{\mathbf{D}} = \omega_{\mathbf{D}}/2\pi = 580$ MHz is the vortex eigenfrequency) [21,22] is shown in Fig. 1(b). The orbital trajectories of the earlier transient and steady-state motions of the initial up core and its reversed down core, and their velocities following their individual orbital trajectories are revealed. It is numerically found that the up-core switches to the down-core when the velocity of the up-core motion reaches a threshold velocity, $v_{\text{cri}}^{\text{Py}} = 330$ m/s for the Py dot, as seen in the right panel of Fig. 1(b), and in our earlier works [9,12,13].

To examine the universality of this value of $v_{\text{cri}}^{\text{Py}} = 330$ m/s, we conducted additional simulations to obtain the VC velocity-versus-time curves varying both H_0 (10 to 350 Oe) and $\nu_{\mathbf{H}}$ (0.1 to 2 GHz) for a Py dot of $R = 150$ nm and $L = 20$ nm, as shown in Fig. 2(a). It is established that the value of $v_{\text{cri}}^{\text{Py}} = 330 \pm 37$ m/s is neither affected by the external field parameters of $\nu_{\mathbf{H}}$ and H_0 nor by the size of the Py dot, as evidenced by the independence of v_{cri} on the dot radius and thickness [Fig. 2(b)]. Furthermore, in order to examine whether any of the intrinsic material parameters affects the value of $v_{\text{cri}}^{\text{Py}}$, we performed simulations for a

circular dot of $R = 150$ nm and $L = 20$ nm, according to artificially varying M_s (the saturation magnetization), A_{ex} , and γ (the gyromagnetic ratio), using $M_s/M_{s,\text{Py}} = 1.0 \sim 2.0$, $(A_{\text{ex}}/A_{\text{ex,Py}})^{1/2} = 0.75 \sim 1.5$, and $\gamma/\gamma_{\text{Py}} = 0.5 \sim 1.75$, where $M_{s,\text{Py}} = 860$ emu/cm³, $A_{\text{ex,Py}} = 1.3$ $\mu\text{erg/cm}$, $\gamma_{\text{Py}} = 2.8 \times 2\pi$ MHz/Oe for Py. The simulation results in Figs. 2(c) and 2(d) display a linear increase of v_{cri} with $(A_{\text{ex}}/A_{\text{ex,Py}})^{1/2}$ with an equal slope for different values of M_s , and a linear increase with $\gamma/\gamma_{\text{Py}}$, respectively.

All the simulation results confirm an explicit analytical form of the critical velocity, $v_{\text{cri}} \simeq \eta \gamma \sqrt{A_{\text{ex}}}$ with the proportional constant $\eta = 5/3 \pm 0.18$. To check the universality of this constant for different magnetic materials, we also simulated the VC switching for various materials such as Ni, Fe, and Co. The values of $\eta_{\text{Fe}} = 1.72 \pm 0.09$, $\eta_{\text{Co}} = 1.71 \pm 0.09$ and $\eta_{\text{Ni}} = 1.91 \pm 0.24$ for these materials are obtained using the corresponding critical velocities, $v_{\text{cri}}^{\text{Fe}} = 439 \pm 22$, $v_{\text{cri}}^{\text{Co}} = 355 \pm 18$, $v_{\text{cri}}^{\text{Ni}} = 320 \pm 40$ m/s, as shown in the inset of Fig. 2(a). All η values are close to $5/3$ and thus identical within the estimated errors. The $\eta = 5/3$ acts as an universal constant that relates the critical velocity for the VC switching and only the parameters of A_{ex} and γ . Moreover, it is interesting that the equation for $v_{\text{cri}} \simeq \frac{5}{3} \gamma \sqrt{A_{\text{ex}}}$ does not explicitly include M_s . This fact can be understood from the physical origin of the VC switching. As reported previously [13], the VC switching is induced by the gyrofield that originates from a dynamic deformation of \mathbf{M} being concentrated around the moving VC. The resultant \mathbf{M} deformation leads to a VC instability and eventually to the VC

switching via pure dynamic processes of the nucleation and annihilation of a vortex-antivortex (V-AV) pair [5-7]. Owing to the dramatic \mathbf{M} deformation employed over a ten nm length scale, the dominant contribution to the critical value of gyrofield is the short-range exchange interaction. Therefore, A_{ex} is the dominant parameter in determining the critical gyrofield and in turn v_{cri} . Following the same argument, the long-range dipolar interaction gives a negligible contribution to v_{cri} , so that the dimensions and shape of a given dot, as well as M_s do not affect the value of v_{cri} , as manifested itself in the equation $v_{\text{cri}} \simeq \frac{5}{3} \gamma \sqrt{A_{\text{ex}}}$.

On the basis of the above results, v_{cri} only depends on A_{ex} , but neither on the dot size nor the driving force parameters of ω_{H} and H_0 . Consequently, we can construct phase diagrams of the VC switching criterion and switching times with respect to ω_{H} and H_0 . Figure 3 shows the simulation results on the switching boundary diagram where the VC switching (gray) and non-switching (white) areas are differentiated by different symbols for the several different dimensions of the Py dots, e.g., $[R \text{ (nm)}, L \text{ (nm)}] = [150, 20], [150, 30], [300, 20], \text{ and } [450, 20]$. The switching event boundaries for all different dimensions of the dots form almost the same line, which reflects again the fact that v_{cri} does not vary with the size of a given dot. Owing to the resonant excitation of the VC motions at $\omega_{\text{H}} = \omega_{\text{D}}$, the VC velocity can reach v_{cri} through its gyrotropic motion even it is driven by only an extremely small field amplitude [5,9,10]. Resonant VC motions yield a deep valley on the switching boundary in the vicinity of $\omega_{\text{H}} = \omega_{\text{D}}$, and, thus, the threshold value of H_0 required for the VC switching has a

minimum at $\omega_H = \omega_D$.

In addition, we theoretically derived more general explicit analytical equations representing the switching boundary, which distinguishes the event of the VC switching and non-switching based on the linearized Thiele's equation of motion. A detailed derivation is described in supplementary online material [23]. Here we chose \mathbf{H}_{CCW} necessary for the resonant gyrotropic motion of the up-core and successive core switching to the down-core [9,10,20]. From the general solution of the VC equation of motion in the linear regime, the instantaneous velocity of the up-core motion as a function of time t driven by \mathbf{H}_{CCW} is found as $v(t) = \frac{1}{3}\gamma RH_0 \sqrt{\Omega^2 + F(\Omega, t)} / \sqrt{(1-\Omega)^2 + d^2\Omega^2}$, where $d = -D/|G|$, $G = 2\pi LM_s / \gamma$ is the gyrovector amplitude, $D < 0$ is the damping constant [18], and $\Omega = \omega_H / \omega_D$. The function $F(\Omega, t)$ represents the time variable velocity term of the transient VC motions and has a maximum at $t_m \approx \pi / |\omega_H - \omega_D|$ [23]. This $v(t)$ equation in turn allows us to analytically construct the boundary (RH_0^C) diagram of the VC switching in the Ω - RH_0 plane by putting $v(t) = v_{\text{cri}}$ and $H_0 = H_0^C$, as written by $RH_0^C \approx (3v_{\text{cri}} / \gamma) \sqrt{(1-\Omega)^2 + d^2\Omega^2} / (\Omega + e^{-d\omega_D t_m})$. The numerical calculation of $RH_0^C(\Omega)$ using $v_{\text{cri}}^{\text{Py}} = 330 \pm 37$ m/s is displayed by the yellow-colored area in Fig. 3. On resonance ($\Omega = 1$), the minimum value of RH_0^C is $3dv_{\text{cri}} / \gamma$, where $d = \alpha [1 + \ln(R/R_C)/2]$, α is the Gilbert damping parameter, R_C is the VC radius [24], indicating that $H_0^C(\Omega=1) \sim 3dv_{\text{cri}} / \gamma R$ is the lowest field strength required for the VC switching [25]. The analytical solution (yellow-colored area) is somewhat in discrepancy with

the micromagnetic simulations (symbols), although they are similar in shape/trend. This discrepancy can be associated with the fact that the present simulations of the VC switching imply a nonlinearity of the VC gyrotropic motions when the motions are close to the switching event [26], whereas the above analytical equation of RH_0^C assumes only a linear-regime vortex motion. However, this nonlinear effect could be compensated simply by multiplying a scaling factor $S_F = +1.4$ to the above equation of RH_0^C . Recent experimental results by Curcic *et al.* [10] support well our results. They reported the value of $H_0^C = 3.4$ Oe for a square dot of 500 nm width and 50 nm thickness, which value is in quite good agreement with our estimated value of $H_0^C = 4.1$ Oe from $S_F 3d\nu_{\text{cri}} / \gamma R$ on resonance, considering the dot size of $R = 250$ nm and $L = 50$ nm, and the experimentally measured value of $\nu_{\text{cri}}^{\text{Py}} = 190$ m/s.

Next, we construct a phase diagram of the switching time T_s , i.e., the time period necessary for the VC switching to complete itself from an initial equilibrium VC position. As already reported in Ref. [7], the VC switching occurs through the serial processes of the nucleation and annihilation of a V-AV pair around the initial VC position, following the maximum deformation of the entire \mathbf{M} structure of the VC [7,13]. This process follows just after $\nu(t)$ reaches ν_{cri} through the gyrotropic motion [12]. Accordingly, T_s consists of three different duration times as expressed by $T_s = \Delta t_g + \Delta t_d + \Delta t_{\text{V-AV}}$. The individual times can thus be determined by the three different processes: Δt_g is the time period required for a VC to reach ν_{cri} , Δt_d is the time period between a time when $\nu(t)$ reaches ν_{cri} and a time when a V-AV pair is nucleated,

and Δt_{V-AV} is the time period during which the serial processes of the nucleation and annihilation of the V-AV pair occur until the VC switching is completed. To estimate each value of Δt_g , Δt_d , Δt_{V-AV} , the above indicated successive processes are differentiated according to the definition of each process, as shown in micromagnetic simulations for a Py dot of $R = 150$ nm and $L = 20$ nm (for details, see Ref. [23]). Then, each value of Δt_g , Δt_d , Δt_{V-AV} , and their sum T_s are plotted as a function of H_0 in Fig. 4(a). For the low field strengths ($H_0 < 0.4$ kOe), Δt_g is on the order of a few ns and becomes increased with decreasing H_0 . Note that Δt_g is much longer than both Δt_d (~ 50 ps) and Δt_{V-AV} (~ 30 ps). For the higher field strengths ($H_0 > 0.5$ kOe), however, Δt_g reaches a few ps, being much less than Δt_d and Δt_{V-AV} , according to the simulation results. However, the LLG equation of motion used in the simulations is invalid on this 1 ps time scale, so that all the results below 10 ps are physically meaningless. Consequently, there is no doubt that for $H_0 < 0.4$ kOe T_s is determined by Δt_g , whereas for $H_0 > 0.5$ kOe, T_s is determined by Δt_d in addition to Δt_{V-AV} , i.e. at least ~ 80 ps, only in the range of physically meaningful switching time. From an application point of view, such high field strengths are not necessary for the VC switching when applying the resonance frequency. In other words, in the range of $H_0 < 0.4$ kOe, Δt_g is sufficient to represent T_s . It is very interesting that Δt_g can be calculated using the analytical equation of $\nu(t)$ along with the condition $\nu(t) = \nu_{\text{cri}}$ at $t = \Delta t_g$ and taking into account the nonlinear effects that can be also compensated by the scaling factor S_F . For $\Omega = 1$ and $H_0 > H_0^C$ (non-switching for

$H_0 < H_0^C$), Δt_g is analytically expressed as $\Delta t_g(H_0) = -(d\omega_D)^{-1} \ln(1 - H_0^C/H_0)$, and this numerical solution is compared with the simulation result in Fig. 4(a).

For the case of $\Omega \neq 1$, Δt_g can also be numerically calculated, as shown in Fig. 4(b), e.g. for a Py dot of $R = 150$ nm and $L = 20$ nm. For $H_0 \gg H_0^C$, Δt_g is ~ 1 ps, and does not vary much with ω_H , but this time scale is physically meaningless since the analytical equation is also derived from the LLG equation of motion that is not valid on the ps time scale, as already mentioned. In contrast, as H_0 decreases close to H_0^C , Δt_g markedly increases and varies considerably with ω_H . At $\Omega = 1$, it appears that the lower H_0^C , the longer Δt_g [27]. For faster VC switching, larger values of H_0 and $\omega_H > \omega_D$ are more effective. Since Δt_g of the order of 1 ps for $H_0 > 0.5$ kOe is not meaningful any more, and in such higher field region $\Delta t_d + \Delta t_{V-AV}$ is dominating in the determination of T_s , only the region of $H_0 < 0.4$ kOe or $\Delta t_g < 0.3$ ns in the phase diagram, shown in Fig. 4(b), would be technologically useful in the optimization of driving force parameters that reliably control the ultrafast VC switching.

In conclusion, the critical velocity, $v_{\text{cri}} = \frac{5}{3}\gamma\sqrt{A_{\text{ex}}}$, of the VC gyrotropic motion has been found to serve as the universal criterion for vortex-core switching, e.g. $v_{\text{cri}}^{\text{Py}} = 330 \pm 37$ m/s. Based on this criterion, we derived phase diagrams of the vortex-core switching and the switching time with respect to the frequency and amplitude of circularly rotating field, which provide guidance for practical implementations of a dot array in the vortex states to information storage devices. These phase diagrams are also useful in the design of the dot dimensions and

proper choice of materials as well as to optimize external driving forces for the reliable ultrafast VC switching at extremely low power consumption.

We thank H. Stoll for fruitful discussions. This work was supported by Creative Research Initiatives (ReC-SDSW) of MEST/KOSEF. P.F. was supported by the Director, Office of Science, Office of Basic Energy Sciences, Materials Sciences and Engineering Division, of the U.S. Department of Energy.

References

* To whom all correspondence should be addressed: sangkoog@snu.ac.kr

- [1] A. Hubert, and R. Schäfer, *Magnetic Domains* (Springer-Verlag, Berlin, New York, Heidelberg, 1998).
- [2] S.-K. Kim, J. B. Kortright, and S.-C. Shin, *Appl. Phys. Lett.* **78**, 2742 (2001); S.-K. Kim *et al.*, *Appl. Phys. Lett.* **86**, 052504 (2005).
- [3] T. Shinjo *et al.*, *Science* **289**, 930 (2000); A. Wachowiak *et al.*, *Science* **298**, 577 (2002); J. Miltat and A. Thiaville, *Science* **298**, 555 (2002).
- [4] R. P. Cowburn, *Nature Mater.* **6**, 255 (2007); J. Thomas, *Nature Nanotech.* **2**, 206 (2007).
- [5] B. Van Waeyenberge *et al.*, *Nature* **444**, 461 (2006).
- [6] R. Hertel, S. Gliga, M. Fähnle, and C. M. Schneider, *Phys. Rev. Lett.* **98**, 117201 (2007). Q. F. Xiao *et al.*, *J. Appl. Phys.* **102**, 103904 (2007).

- [7] K.-S. Lee, K. Y. Guslienko, J.-Y. Lee, and S.-K. Kim, Phys. Rev. B **76**, 174410 (2007).
- [8] V. P. Kravchuk *et al.*, J. Appl. Phys. **102**, 043908 (2007).
- [9] S.-K. Kim, K.-S. Lee, Y.-S. Yu, and Y.-S. Choi, Appl. Phys. Lett. **92**, 022509 (2008).
- [10] M. Curcic *et al.*, Phys. Rev. Lett. (in press).
- [11] K. Yamada *et al.*, Nature Mater. **6**, 269 (2007).
- [12] S.-K. Kim *et al.*, Appl. Phys. Lett. **91**, 082506 (2007).
- [13] K. Y. Guslienko, K.-S. Lee, and S.-K. Kim, Phys. Rev. Lett. **100**, 027203 (2008).
- [14] B. Krüger *et al.*, Phys. Rev. B **76**, 224426 (2007); M. Bolte *et al.*, Phys. Rev. Lett. **100**, 176601 (2008).
- [15] S.-K. Kim, K.-S. Lee, Y.-S. Choi, and Y.-S. Yu, IEEE Trans. Magn. (in press).
- [16] See <http://math.nist.gov/oommf>.
- [17] L. D. Landau and E. M. Lifshitz, Phys. Z. Sowjet. **8**, 153 (1935); T. L. Gilbert, Phys. Rev. **100**, 1243 (1955).
- [18] A. A. Thiele, Phys. Rev. Lett. **30**, 230 (1973); D. L. Huber, Phys. Rev. B **26**, 3758 (1982).
- [19] A linearly oscillating field can be decomposed into the CCW and clockwise (CW) rotating fields with the equal H_0 and ω_H values [9].
- [20] K.-S. Lee and S.-K. Kim, Phys. Rev. B **78**, 014405 (2008).
- [21] K. Y. Guslienko *et al.*, J. Appl. Phys. **91**, 8037 (2002).
- [22] J. P. Park *et al.*, Phys. Rev. B **67**, 020403(R) (2003); S. B. Choe *et al.*, Science **304**, 420

(2004); K. Y. Guslienko *et al.*, Phys. Rev. Lett. **96**, 067205 (2006).

[23] See EPAPS Document No. XXX for detailed descriptions. For more information on EPAPS, see <http://www.aip.org/pubservs/epaps.html>.

[24] K. Y. Guslienko, Appl. Phys. Lett **89**, 022510 (2006).

[25] For CW rotating fields, RH_0^C has a constant value of $3\nu_{\text{cri}}/\gamma$, which indicates that the RH_0^C value of the \mathbf{H}_{CW} is much larger than that of \mathbf{H}_{CCW} .

[26] K.-S. Lee and S.-K. Kim, Appl. Phys. Lett **91**, 132511(2007); K. S. Buchanan *et al.*, Phys. Rev. Lett. **99**, 267201 (2007).

[27] From micromagnetic simulation results for $R = 150$ nm (300 nm) and $L = 20$ nm, H_0^C is only 14 Oe (7 Oe) and T_s is 17 ns (33 ns).

FIG. 1 (color online). (a) Magnetic vortex structure with either upward or downward core \mathbf{M} orientation. The rotation sense of the local in-plane \mathbf{M} around the VC is CCW. (b) The orbital trajectories (left) and velocity-versus-time curves of the up (red line) and down (blue line) cores in a circular Py nanodot of $R = 150$ nm and $L = 20$ nm driven by the indicated \mathbf{H}_{CCW} of $\omega_{\text{H}} / \omega_{\text{D}} = 1$ and $H_0 = 20$ Oe. Also, the velocities of VC motions driven by \mathbf{H}_{CW} and \mathbf{H}_{Lin} are plotted for comparison. The horizontal line (right) denotes the value of $v_{\text{cri}}^{\text{Py}} = 330$ m/s with an estimated error of ± 37 m/s (gray-color region)

FIG. 2 (color online). (a) Instantaneous VC velocity $v(t)$ in the Py dot of $R = 150$ nm and $L = 20$ nm for different values of H_0 and $\Omega = \omega_{\text{H}} / \omega_{\text{D}}$. The inset shows the VC velocities versus time for different dots made of Fe, Co, and Ni. (b), (c), and (d) show the dependences of v_{cri} on the dimensions of the Py dot, the material parameters of A_{ex} , M_{s} , and γ , respectively. All the results were obtained from the micromagnetic simulations. The gray-colored regions with the lines indicate the value of v_{cri} with its error range ± 37 m/s.

FIG. 3 (color online). The boundary diagram of the VC switching driven by the field \mathbf{H}_{CCW} in the $\Omega - RH_0$ plane. Blue circle, green triangle, orange square and black diamond symbols correspond to the simulated results for $[R \text{ (nm)}, L \text{ (nm)}] = [150, 20], [150, 30], [300, 20],$ and $[600, 20],$ respectively. Yellow (dark gray) colored area indicates the switching boundary

obtained using the analytical equation of RH_0^C shown in the text for Py dots with $R = 50 \sim 5000$ nm and $L = 20 \sim 80$ nm, based on the estimated value of $v_{\text{cri}}^{\text{Py}} = 330 \pm 37$ m/s. The light purple (gray) colored area is the result of the multiplication of $S_F = 1.4$ to the equation of RH_0^C . The left side (blue-colored) axis indicates the result corresponding to specific dimensions, $[R \text{ (nm)}, L \text{ (nm)}] = [150, 20]$.

FIG. 4 (color online). (a) Time periods for the individual indicated processes as a function of the amplitude H_0 of \mathbf{H}_{CWW} at $\omega_{\text{H}}/2\pi = \omega_{\text{D}}/2\pi = 580$ MHz, obtained from micromagnetic simulations (symbols with lines) for a Py dot of $R = 150$ nm and $L = 20$ nm, being compared with the numerical calculation (line) of the analytical form of Δt_g . (b) Contour plot of the VC switching time in the $\Omega - H_0$ plane, obtained from the numerical calculation of Δt_g for the Py dot with $R = 150$ nm and $L = 20$ nm. Δt_g values only in the region below the indicated white dashed line represents T_s .

FIG.1.

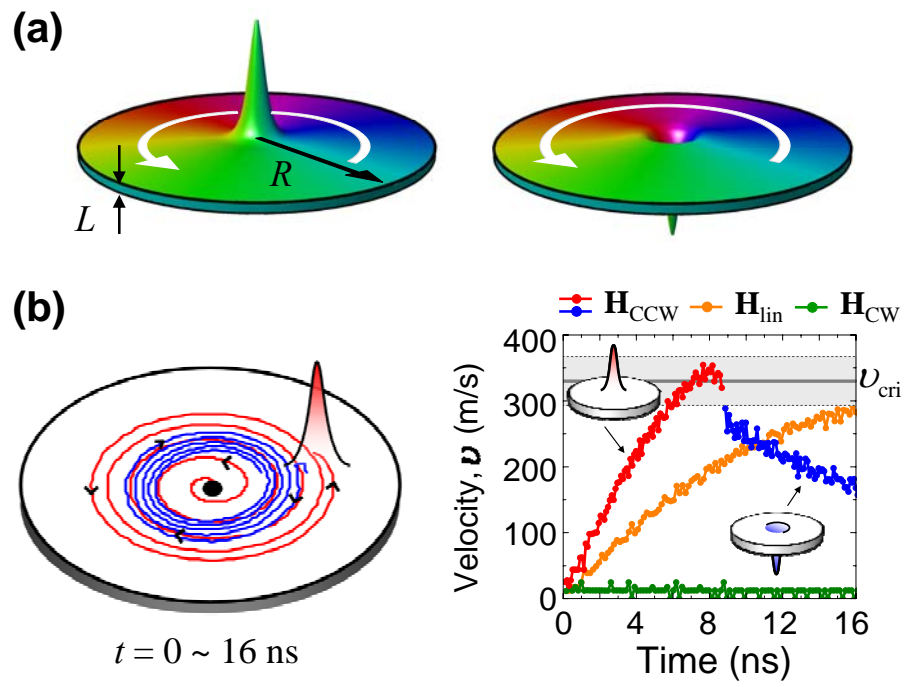


FIG.2.

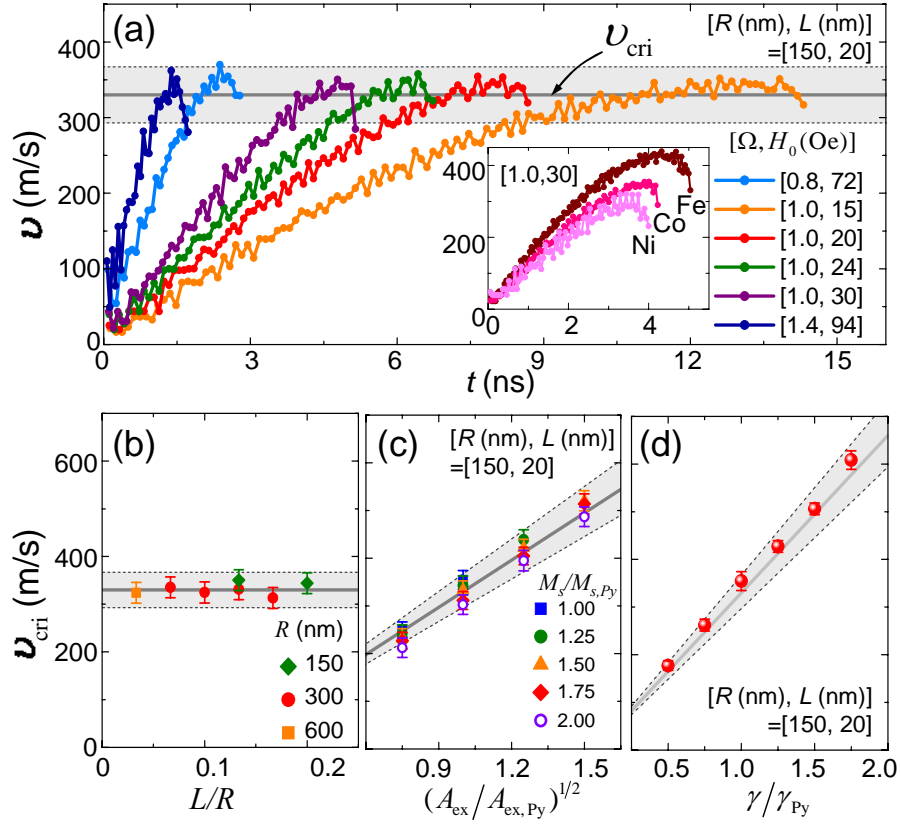


FIG.3.

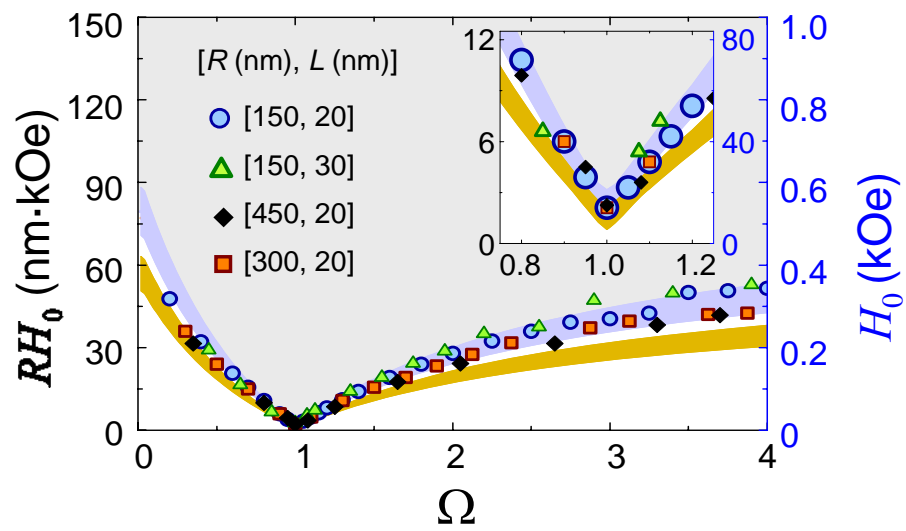
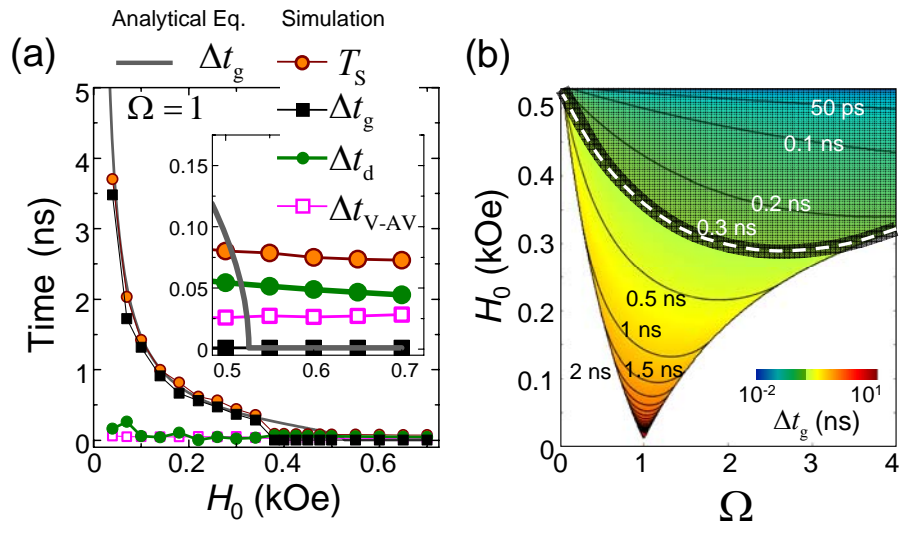


FIG.4.



Supplementary Documents

A. Derivation of the instantaneous VC velocity, $v(t)$

To analytically derive the velocity of vortex-core motions in the linear regime, we derived the general solution of the vortex-core motion in both the earlier transient and later steady states [S1] based on the linearized Thiele's equation [S2]:

$-\mathbf{G} \times \dot{\mathbf{X}} - \hat{D}\dot{\mathbf{X}} + \partial W(\mathbf{X}, t)/\partial \mathbf{X} = 0$ with the vortex-core position $\mathbf{X} = (X, Y)$, the gyrovector $\mathbf{G} = -G\hat{\mathbf{z}}$, the damping tensor $\hat{D} = D\hat{I}$ (the identity matrix \hat{I} and the damping constant $D < 0$), and the potential energy function $W(\mathbf{X}, t)$ [S1, S3]. To solve the elementary rotating eigenmotions of a vortex core in a circular dot driven by the counter-clockwise (CCW)- and clockwise (CW)-circular rotating fields (\mathbf{H}_{CCW} and \mathbf{H}_{CW}) [S4, S5], it is useful to utilize a complex variable $S \equiv X + iY$ for a vortex-core position $\mathbf{X} = (X, Y)$ at a time t , where the real and imaginary values indicate the x - and y -positions of the vortex core, respectively. For the case of applications of \mathbf{H}_{CCW} for a selective switching from the up- to down-core, the general solution in the linear regime is given as $S = [S(0) - S_0] \exp(i\omega_{\text{D}}t) \exp(-d\omega_{\text{D}}t) + S_0 \exp(i\omega_{\text{H}}t)$ [S6] with $d = -D/|G|$ and $\omega_{\text{D}} = \kappa|G|/(G^2 + D^2)$ [S4, S5], where κ is the stiffness coefficient of the potential energy $W(S, t)$, $S_0 = i\mu H_0/(\kappa - \omega_{\text{H}}G - i\omega_{\text{H}}D)$, and $S(0) = X_0 + iY_0$. $\mathbf{X}(0) = (X_0,$

Y_0) corresponds to the initial vortex-core position in an equilibrium state at $t = 0$. From the time derivative of this general solution of the vortex-core position \mathbf{X} , the velocity of the up-core motion driven by \mathbf{H}_{CCW} is written as

$$v(t) = \frac{1}{3} \gamma R H_0 \frac{\sqrt{\Omega^2 + F(\Omega, t)}}{\sqrt{(1 - \Omega)^2 + d^2 \Omega^2}}$$

with the transient term of

$$F(\Omega, t) = \exp(-2d\omega_d t) - 2\Omega \exp(-d\omega_d t) \left[\cos((1 - \Omega)\omega_d t) - d \left[\sin((1 - \Omega)\omega_d t) \right] \right] ,$$

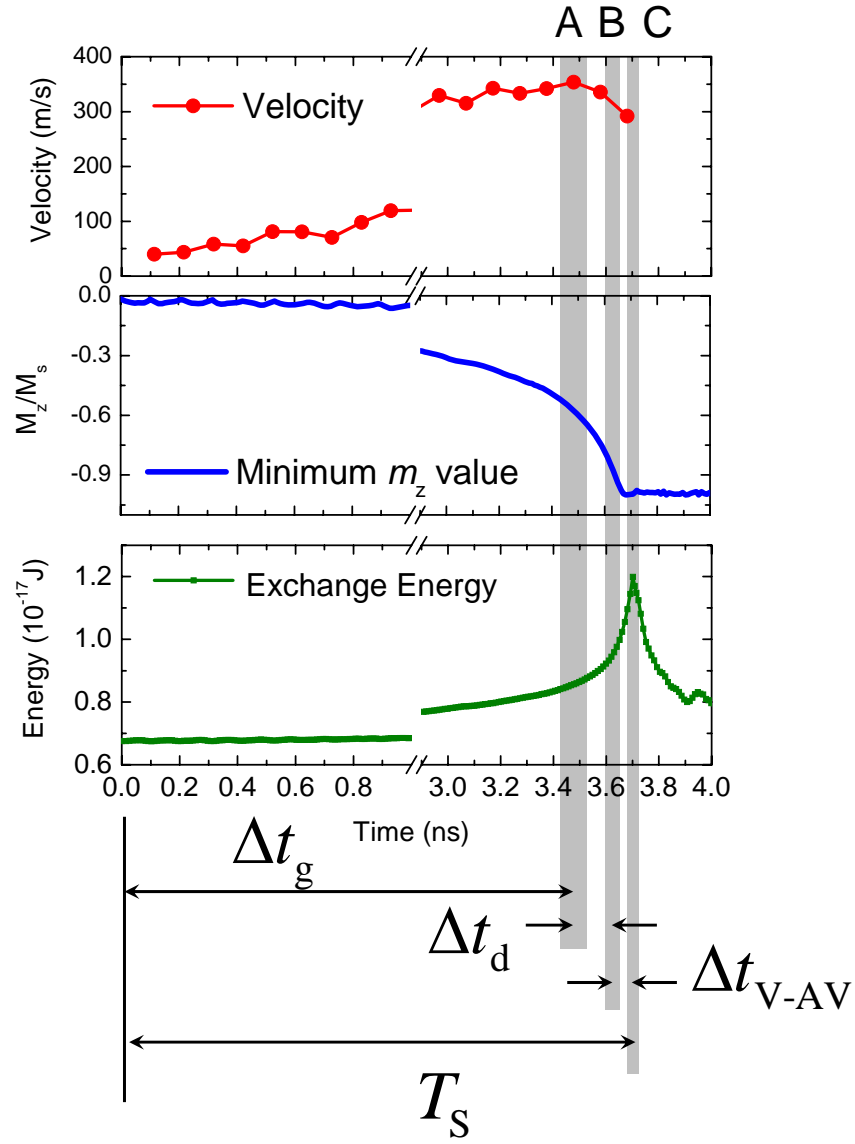
where $\Omega = \omega_H / \omega_D$. For a sufficiently large value of t , the function $F(\Omega, t)$ converges to 0, i.e., the vortex motions arrive at certain pure steady states and the earlier transient states disappear.

B. Entire switching time T_s for complete vortex-core switching

Ultrafast vortex-core switching in a soft magnetic nanodot is known to take place through the serial processes of the nucleation and annihilation of a vortex-antivortex pair around the initial vortex-core position [S7], following the maximum deformation of the entire magnetization structure of the initial vortex core [S7,S8]. This maximization of vortex-core deformation can be established just after the vortex-core velocity reaches its threshold velocity v_{cri} through its characteristic gyrotropic motion [S9]. Thereby, the entire switching time T_s , necessary for the vortex-core switching to complete itself from an initial equilibrium vortex-core position, consists of three different duration times, which are determined by the three different individual processes described above, such that, $T_s = \Delta t_g + \Delta t_d + \Delta t_{\text{V-AV}}$. Δt_g is the time period required for a vortex-core to reach v_{cri} through the gyrotropic motion, Δt_d is the time period during which a dynamic deformation of the entire magnetization of the initial vortex core is maximized before the nucleation process of a vortex-antivortex pair starts and after the initial vortex-core velocity reaches v_{cri} , and $\Delta t_{\text{V-AV}}$ is the time period during which the serial processes of the nucleation and annihilation of a vortex-antivortex pair take place until vortex-core switching is completed.

To obtain the entire switching time T_s for complete vortex core switching as a function of the field amplitude and frequency of counter-clockwise circularly rotating magnetic fields, it is necessary to define each boundary between the individual successive processes. Supplementary Figure 1 shows the three different duration times, obtained from micromagnetic simulations for vortex-core switching from the up- to

down-core in a Permalloy dot of $R = 150$ nm and $L = 20$ nm, driven by a counter-clockwise rotating field of $H_0 = 40$ Oe and $\omega_{\text{H}}/2\pi = \omega_{\text{D}}/2\pi = 580$ MHz. Each boundary between the successive two processes is indicated by the thick gray-colored vertical lines. The three different boundaries are denoted as “A”, “B”, and “C” in Suppl. Fig. 1 (the thick lines indicate the corresponding errors). The “A” represents when the instantaneous velocity $v(t)$ reaches v_{cri} , “B” indicates when the minimum value of the out-of plane magnetization component m_z , which represents the degree of deformation [S8], reaches -0.9 for the up- to down-core switching, and “C” denotes when the exchange energy reaches its maximum (this energy term is maximized when the vortex-antivortex pair is annihilated [S7]).



SUPPL. FIG. 1. Duration times necessary for the individual processes for complete vortex-core switching and boundaries between the individual successive processes. The results were obtained from micromagnetic numerical calculations for a Permalloy dot of $R = 150$ nm and $L = 20$ nm, and the CCW circularly rotating field with $H_0 = 40$ Oe and $\nu_H = \nu_D = 580$ MHz.

References

- [S1] K.-S. Lee and S.-K. Kim, Appl. Phys. Lett. **91**, 132511 (2007).
- [S2] A. A. Thiele, Phys. Rev. Lett. **30**, 230 (1973); D. L. Huber, Phys. Rev. B **26**, 3758 (1982).
- [S3] K. Y. Guslienko, V. Novosad, Y. Otani, H. Shima, and K. Fukamichi, Phys. Rev. B **65**, 024414 (2002); K. Y. Guslienko, Appl. Phys. Lett. **89**, 022510 (2006).
- [S4] K.-S. Lee and S.-K. Kim, Phys. Rev. B **78**, 014405 (2008).
- [S5] S.-K. Kim, K.-S. Lee, Y.-S. Yu, and Y.-S. Choi, Appl. Phys. Lett. **92**, 022509 (2008).
- [S6] K.-S. Lee and S.-K. Kim (unpublished).
- [S7] K.-S. Lee, K. Y. Guslienko, J.-Y. Lee, and S.-K. Kim, Phys. Rev. B **76**, 174410 (2007).
- [S8] K. Y. Guslienko, K.-S. Lee, and S.-K. Kim, Phys. Rev. Lett. **100**, 027203 (2008).
- [S9] S.-K. Kim, Y.-S. Choi, K.-S. Lee, K. Y. Guslienko, and D.-E. Jeong, Appl. Phys. Lett. **91**, 082506 (2007).